Nuclear Science and Techniques (2025) 36:168
https://doi.org/10.1007/s41365-025-01763-8

DATA ARTICLE

New measurement of ^{165}Ho neutron capture cross sections

Su-Ya-La-Tu Zhang[1,2] · Yong-Shun Huang[1,2] · Wei Jiang[3,4] · Jie Ren[5] · Rui-Rui Fan[3,4] · De-Xin Wang[1,2] · Chun-Lei Zhang[6] · Guo Li[1,2] · Dan-Dan Niu[1,2] · Mei-Rong Huang[1,2]

Received: 18 February 2025 / Revised: 9 April 2025 / Accepted: 10 April 2025 / Published online: 29 June 2025

Abstract

The neutron capture cross section for ^{165}Ho was measured at the backstreaming white neutron beam line (Back-n) of the China Spallation Neutron Source (CSNS) using total energy detection systems, composed of a set of four C_6D_6 scintillator detectors coupled with pulse height weighting techniques. The resonance parameters were extracted using the multilevel multichannel R-matrix code SAMMY to fit the measured capture yields of the ^{165}Ho(n,γ) reaction in the neutron energy range below 100 eV. Subsequently, the resonance region's capture cross sections were reconstructed based on the obtained parameters. Furthermore, the unresolved resonance average cross section of the ^{165}Ho(n,γ) reaction was determined relative to that of the standard sample ^{197}Au within the neutron energy range of 2 keV to 1 MeV. The experimental data were compared with the recommended nuclear data from the ENDF/B-VIII.0 library, as well as with results of calculations performed using the TALYS−1.9 code. The comparison revealed agreement between the measured ^{165}Ho(n,γ) cross sections and these data. The present results are crucial for evaluating the ^{165}Ho neutron capture cross section and thus enhance the quality of evaluated nuclear data libraries. They provide valuable guidance for nuclear theoretical models and nuclear astrophysical studies.

Keywords Holmium · Neutron capture reaction · Cross section · Total energy detection principle · C_6D_6 scintillator detector · China Spallation Neutron Source

1 Introduction

Nuclear data are used to describe the physical properties of atomic nuclei and their interactions, thus playing a key role in fundamental nuclear physics research and the development of nuclear energy and nuclear technology [1, 2]. Neutron capture cross-sectional data are critical for stellar nucleosynthesis of heavy elements, medical applications, radiation dosimetry, transmutation of nuclear waste, and advanced nuclear energy systems [3–5].

Numerous laboratories worldwide, including CERN n_TOF [6], Los Alamos National Laboratory DANCE [7], Karlsruhe [8], and GELINA [9], have developed two types of detection systems for online measurement of neutron capture cross sections. These systems include γ-ray total energy and total absorption detectors. Total energy detection systems generally use a low-efficiency C_6D_6 scintillator detector, which is suitable for measuring stable nuclei exhibiting large cross sections and requiring the use of large samples. Total absorption detection systems often use a BaF_2 crystal detector array with high energy resolution, good time resolution, low neutron sensitivity, and high efficiency to

This work was supported by the National Natural Science Foundation of China (Nos.12465024, 12365018, U2032146), Inner Mongolia National Science Foundation (Nos. 2024ZD23, 2024FX30, 2023MS01005), Program for Innovative Research Team in Universities of Inner Mongolia Autonomous Region (NMGIRT2217), Program for Young Talents of Science and Technology in Universities of Inner Mongolia Autonomous Region (NJYT23109).

✉ Su-Ya-La-Tu Zhang
zsylt0416@163.com

1 College of Physics and Electronic Information, Institute of Nuclear Physics, Inner Mongolia Minzu University, Tongliao 028000, China

2 Inner Mongolia Joint Key Laboratory for Nuclear and Radiation Detection, Tongliao 028000, China

3 Institute of High Energy Physics, Chinese Academy of Sciences, Beijing 100049, China

4 Spallation Neutron Source Science Center, Dongguan 523803, China

5 China Institute of Atomic Energy, Beijing 102413, China

6 College of Nuclear Science and Technology, Beijing Normal University, Beijing 100191, China

perform neutron capture measurements for small-sized samples, small cross sections, and unstable radio nuclides. The China Spallation Neutron Source (CSNS) [10] produces neutrons by bombarding a high-intensity 1.6-GeV proton beam on a tungsten target. The backstreaming neutron beam line (Back-n) is positioned in the reverse direction of the proton beam at the CSNS, with a flight pass length of approximately 76 m. Figure 1 illustrates a schematic view of the experimental setup of the CSNS Back-n. Currently, five types of spectrometers are being constructed at the Back-n facility for nuclear data measurements. These instruments include a set of four C_6D_6 detectors [11–13] and a 4π BaF_2 detector array, referred to as the Gamma Total Absorption Facility II (GTAF-II) [14], which will be utilized for neutron capture measurements. In addition, a multilayer fast ionization chamber (FIXM) is employed for fission reaction measurements [15], and a neutron total cross-sectional detector (NTOX) has been specifically designed for total cross-sectional measurements [16]. Furthermore, light-charged particle detectors are used to measure light-charged particle emissions [17]. A detailed description of the spectrometers is provided in Refs. [18].

Holmium (composed entirely of the isotope ^{165}Ho with 100% natural abundance) has been proposed as the standard for neutron capture cross-sectional measurements owing to its favorable radioactive half-life and large capture cross section observed at the first resonance peak, which is essential for "saturation resonance" calibration [19–21]. Previous studies on ^{165}Ho(n, γ) have revealed notable discrepancies. Poenitz et al. [22, 23] have reported divergent keV–MeV cross sections determined using time-of-flight (TOF) and statistical models, and Voignier et al. [24] have identified data scarcity for holmium. Recently reported Oslo method analyses [25] reduce MACS uncertainties; however, they highlight unresolved impacts of low-energy isomers on *s*-process abundances. Therefore, extensive neutron capture measurements of ^{165}Ho are required to test the accuracy of the evaluated nuclear data and available experimental data. This paper presents a new dataset of the ^{165}Ho(n, γ)^{166}Ho reaction in the neutron energy range from 1 eV to 1 MeV, measured using the C_6D_6 detection system at the CSNS Back-n white neutron source. In the following sections, we outline the methods employed in the experiment and data analysis, discuss the reliability of the results, and provide detailed information on the CERN ROOT code [26] relevant to this study.

2 Methods

2.1 Measurements

In May 2022, the ^{165}Ho(n, γ)^{166}Ho reaction was measured in the CSNS Back-n experimental area (#ES2), which has a flight path length of approximately 76 m. The neutron beam, with ϕ30 mm beam spots, was delivered at ES2 with approximately 6.92×10^5 cm^{-2}s^{-1} neutrons per nominal pulse of 1.6×10^{13} protons in the energy range from 0.3 eV to 200 MeV. The neutron energy spectrum was determined using two different detectors, viz. a Li–Si detector and a calibrated fission chamber, with working principles based on the ^{6}Li(n, t) and ^{235}U(n, f) reactions, respectively [27, 28]. The neutron flux in the experiment was monitored using a silicon flux monitor (SiMon) comprising a thin ^{6}LiF conversion layer and eight silicon detectors; the SiMon was installed approximately 20 m upstream from the sample location. The γ-rays from the ^{165}Ho capture reaction were detected using a set of four C_6D_6 scintillators. These detectors were positioned approximately 17 cm away from the target at an angle of 125° relative to the

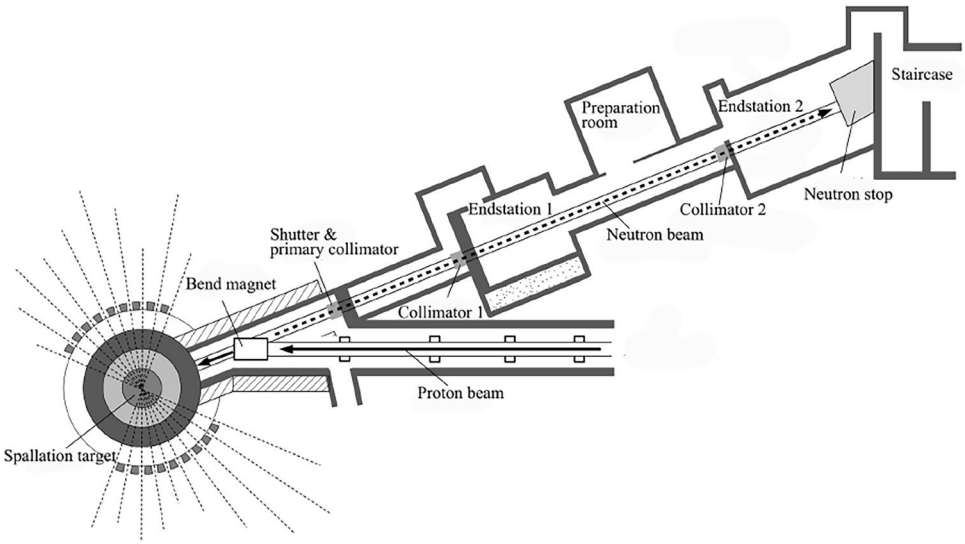

Fig. 1 (Color online) Schematic view of the experimental setup of the CSNS Back-n [18]

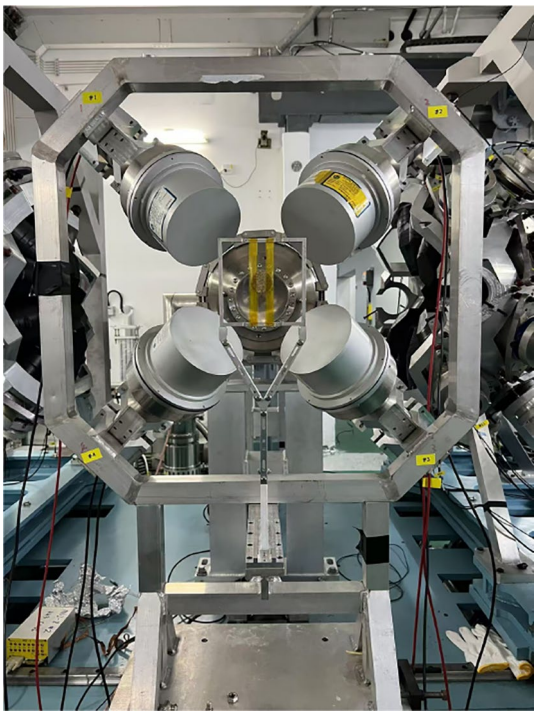

Fig. 2 (Color online) Setup of the four C_6D_6 detectors in the measurement. The detectors were positioned approximately 17 cm away from the target at an angle of 125° relative to the neutron beam

Table 1 Characteristic parameters of samples

Sample	Thickness (mm)	Diameter (mm)	Mass (mg)	Area density (atom · b^{-1})
^{165}Ho	0.20	30	1243.32	6.42×10^{-4}
^{197}Au	0.10	30	1357.17	5.87×10^{-4}
^{nat}Pb	0.53	30	4249.75	1.75×10^{-3}
Empty holder				

neutron beam (Fig. 2). The characteristics of the samples used in this experiment were provided by the China Institute of Atomic Energy (Table 1). A natural metallic holmium sample was used to determine the neutron capture cross section of ^{165}Ho, whereas a gold sample was used to measure the neutron flux and normalize the neutron capture data. Background signals due to scattered neutrons and in-beam γ-rays were measured using a lead sample. Additionally, an empty sample run was performed to evaluate the sample-independent background. The detector signals were recorded using the CSNS Back-n general-purpose data acquisition system [29], which was operated at a sampling rate of 1 GS/s with 12-bit full-waveform digitizers. Data acquisition was triggered by a pickup signal from the proton beam. Dead time corrections were disregarded owing to the lower event statistics observed in this experiment. The total beam measurement time was 100 h, and the offline analysis was performed using the CERN ROOT code.

2.2 Data analysis

The ^{nat}Pb sample data were parameterized using Eq.(1) to evaluate the in-beam γ-ray and scattered neutron background contributions. The ^{165}Ho sample, with ^{181}Ta and ^{59}Co neutron filters, was used to determine the normalization factors f_n and f_γ for the B_n and B_γ components by matching the dips of the filtered spectra. The influence of the filters on the in-beam γ -rays and neutrons was carefully assessed by analyzing the neutron flux and energy distribution of the in-beam γ-rays [30]. The energy spectra of the neutrons and γ-rays produced at the spallation target were randomly sampled to analyze the incident particle energy spectra using the GEANT4 Monte Carlo code [31]; this step allowed simulations both with and without filters. The counts of the scattered neutrons and γ-rays were recorded at the detector position. The reduced attenuation factors for neutrons and γ-rays are found to be 0.92 and 0.68 [12], respectively, which are applied as corrections to f_n and f_γ. Further information on the evaluation method used in this study is reported elsewhere [12].

$$B(E_n) = f_\gamma B_\gamma(E_n) + f_n B_n(E_n) \tag{1}$$

where B_γ and B_n denote the background contributions of the in-beam γ-rays and scattered neutrons, respectively, and can be formulated using Eqs. (2–3).

$$B_\gamma(E_n) = b \times e^{-c/\sqrt{E_n}} + d \times e^{-e\times\sqrt{E_n}} + f \tag{2}$$

$$B_n(E_n) = \frac{a}{\sqrt{E_n}} \tag{3}$$

The experimental neutron capture yield can be calculated as a function of neutron energy using Eq. (4).

$$Y_{exp}(E_n) = \frac{1}{f_n}\frac{S(E_n) - B(E_n)}{\epsilon_c \times \Phi(E_n)} \tag{4}$$

where E_n is the incident neutron energy converted from the neutron TOF spectra by using a relativistic relationship; $S(E_n)$ is the ^{165}Ho sample count; $B(E_n)$ is the evaluated background; and $\Phi(E_n)$ is the neutron flux. The normalization factor f_n, determined by self-normalizing the measured capture yield of the 4.9-eV resonance of ^{197}Au, accounts for the absolute incident neutron flux. ϵ_c is the detection efficiency for a captured event. The total energy detection principle was utilized by combining the aforementioned C_6D_6 detection system with the pulse height weighting technique (PHWT) [32, 33] to achieve proportionality between ϵ_c and the total γ-ray energy (E_c) released in the capture event.

Therefore, we can express $\epsilon_c = kE_c = k(S_n + E_{cm})$, where S_n is the neutron separation energy (6.24 MeV) of the compound nucleus, E_{cm} is the center of mass energy of the incident neutron, and the proportionality factor k is set as 1 MeV^{-1}. In the analysis of the $^{165}Ho(n,\gamma)^{166}Ho$ measurements, the established thresholds were $E_{dep}^{min} = 250$ keV and $E_{dep}^{max} = 7$ MeV, corresponding to the Compton edges for γ-ray energies of 124 keV and 6.75 MeV, respectively. The weighted function (WF), as a 5th-order polynomial function, was fitted using the Geant4 Monte Carlo code to simulate the C_6D_6 detector's response for 27 different monoenergetic γ-rays from 0.1 MeV to 10 MeV. This WF was then applied to all the $S(E_n)$ and $B(E_n)$ spectra for data analysis.

The resonance shape analysis code SAMMY [34] was used to fit the measured neutron capture yield with Eqs. (4). In the SAMMY code, the reaction cross section is described by a multilevel multichannel Reich–Moore formalism, which only depends on the properties of the nuclear excitation state. This code considers all experimental conditions, such as multiple interacting events, sample characteristics, self-shielding, broadening of resonances due to thermal motion, and the experimental resolution of the CSNS Back-n facility [35]. During the fitting process, the initial resonance parameters were obtained from the evaluated nuclear data library ENDF/B-VIII.0 [36] and iteratively refined until convergence. The resonance parameters, including the resonance energy and capture kernels, were determined by SAMMY fitting within the resonance region up to 100 eV, where individual neutron resonances were fitted with high precision. Based on these resonance parameters, the resonance cross sections for the $^{165}Ho(n,\gamma)^{166}Ho$ reaction were reconstructed. However, the resonance structures could not be adequately resolved beyond approximately 100 eV because of deterioration in the experimental resolution and reduced event statistics with increasing neutron energy. Consequently, an average neutron capture cross section was directly derived from the measured neutron capture yield in the unresolved resonance range using 5 (where N_s represents the areal density of the sample). In this case, the measured capture yield was corrected for multiple scattering and self-shielding effects using the Geant4 code, which accounted for sample composition, geometry, and both neutron scattering and capture cross sections. Subsequently, the ^{165}Ho neutron capture cross section was determined relative to that of the standard ^{197}Au sample [37] within the neutron energy range from 2 keV to 1 MeV.

$$\sigma_\gamma = \frac{Y_{exp}(E_n)}{N_s} \tag{5}$$

The uncertainties in the experimental data were attributed to both statistical and systematic errors. The systematic errors were evaluated based on the contributions from various sources, including the energy-dependent neutron flux shape (4.5% below 150 keV and 8.0% above this threshold), normalization (1%), background subtraction using filters (approximately 8.6%), sample impurities (0.01%), and the calculation of PHWT (3%). The sum of these components yielded an overall systematic uncertainty of 10.2%(12.2%) for the capture cross section.

3 Data records

For each neutron pulse, the data from three different types of detectors were recorded and stored simultaneously. The first type is a proton beam counter, which is monitored by the pickup detector of the Proton Synchrotron accelerator. The second type was a neutron flux counter composed of eight SiMon detectors. These two data types were utilized for cross-validation and normalization of various measurements. The third type includes event information for the radiative neutron capture recorded by four C_6D_6 scintillator detectors. All the aforementioned data were acquired using the fully digital data acquisition system of the CSNS Back-n [29], with event-by-event connectivity based on the CERN ROOT code. For each neutron capture event, the deposited energy, represented as the pulse height spectrum in the C_6D_6 detector, and TOF information of the incident neutrons were recorded. Table 2 summarizes the event information for all the samples used in the measurements. The data records are organized in a Tree format according to the CERN ROOT version 5.34 and consist of two branch datasets: "NeuDataTree" and "SiDataTree." "NeuDataTree" recorded data from four C_6D_6 detectors, including nine leaves: GPSsec (triggering time in seconds), GPSnsec (triggering time in nanoseconds), T0id (trigger T0 identification number), BCid (detector identification number), Energy (neutron energy spectrum), Tof (time-of-flight spectrum), Ph (pulse height spectrum), PeakValue (pulse amplitude), and PeakPoint (pulse timing information). "SiDataTree," on the other hand, contained data from eight SiMon detectors, organized into six leaves: GPSsec (triggering time in seconds), GPSnsec (triggering time in nanoseconds), T0id (trigger T0 identification number), BCid(detector identification number), SiTof (time-of-flight spectrum), and SiPeakValue

Table 2 Summary of the event information for all the samples

Sample	Measurement time	Document number	Number of files
^{165}Ho	52 h 56 m	15935,15955	1085
^{197}Au	5 h16 m	15927,15946	102
^{nat}Pb	9 h 41 m	15931,15950	182
Empty holder	12 h 48 m	15944,15956	190

(pulse amplitude). This structured organization of data enables efficient storage and facilitates detailed analysis of the time, energy, and spectral characteristics captured by the detectors.

All the raw data described in this paper have been uploaded to the Science Data Bank. A direct link to the dataset is available at (https://doi.org/10.57760/sciencedb.21041).

4 Technical validation

Figure 3 compares the SAMMY fitting results (red lines) with the measured capture yields (black circles), for the ^{165}Ho(n, γ)^{166}Ho reaction, across neutron energy ranges below 100 eV. Good agreement is observed between the measured and SAMMY fitting results, both in terms of resonance energy and spectral shape. The resonance energies E_R, radiative width Γ_γ, neutron width Γ_n, and capture kernels k ($k = g\Gamma_n\Gamma_\gamma/(\Gamma_n + \Gamma_\gamma)$, g is a statistical factor) obtained in this study are compared with the data from the ENDF/B-VIII.0 library [36], as detailed in Table 3. The experimental capture resonance parameters are in good agreement with the ENDF/B-VIII.0 values in the energy range below 100 eV. However, disparities are observed in the energy range between 100 eV and 2 keV due to the degradation of the experimental resolution function encountered at the CSNS Back-n facility during this measurement.

Figure 4 compares the ^{165}Ho(n,γ)^{166}Ho cross sections calculated using TALYS−1.9 [38] with the results reconstructed based on the SAMMY resonance fitting for neutron energies below 100 eV. In Fig. 5, the measured neutron capture cross sections in the energy range of 2 keV to 1 MeV are displayed with the results calculated using TALYS−1.9 and the data derived from the ENDF/B-VIII.0 library [36]. These comparison results demonstrate that the cross sections determined in this study were accurately reproduced by both the TALYS−1.9 calculations and evaluated data across the investigated full neutron energy range. These results confirm that

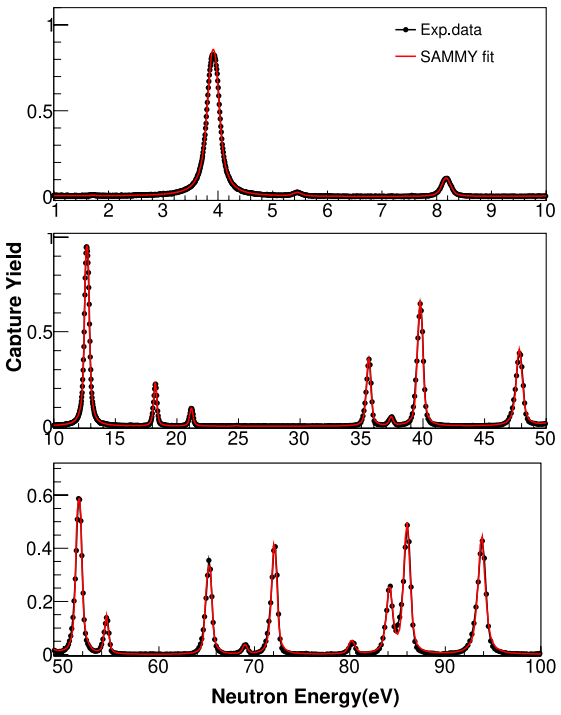

Fig. 3 (Color online) SAMMY fitting (red lines) to the measured capture yields (black circles) of ^{165}Ho(n, γ)^{166}Ho reaction

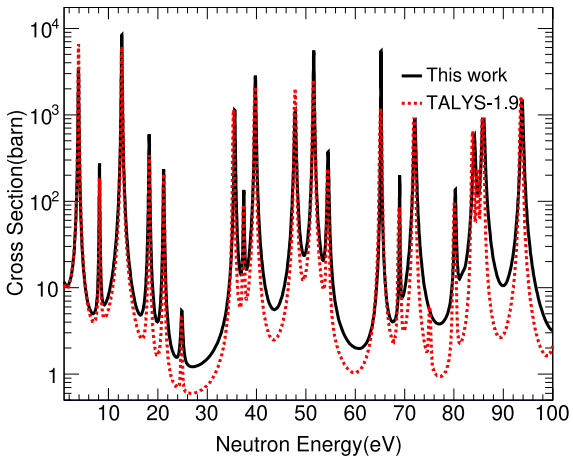

Fig. 4 (Color online) Comparison of ^{165}Ho(n, γ)^{166}Ho cross sections, reconstructed from SAMMY resonance fitting, up to a neutron energy of 100 eV, with the calculations from TALYS code version 1.9 [38]

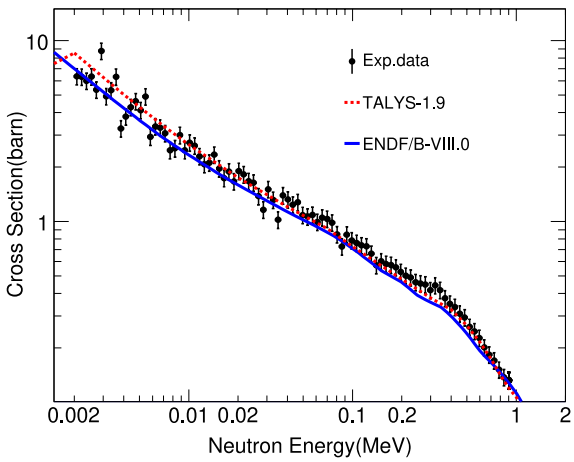

Fig. 5 (Color online) Comparisons of the neutron capture cross section of ^{165}Ho, measured in this study, with the TALYS−1.9 calculations [38] and ENDF/B-VIII.0 evaluated data [36] from 2 keV to 1 MeV

Table 3 Resonance parameters up to a neutron energy of 100 eV for the ^{165}Ho (n, γ) cross sections

J	This work				ENDF/B-VIII.0			
	E_R (eV)	Γ_n (meV)	Γ_γ (meV)	k	E_R (eV)	Γ_n (meV)	Γ_γ (meV)	k
4	3.91 ± 0.01	1.28 ± 0.01	129.10 ± 0.13	0.71 ± 0.01	3.91	2.13	85.70	1.17
3	8.17 ± 0.02	0.20 ± 0.01	98.66 ± 0.06	0.09 ± 0.01	8.17	0.19	90.30	0.08
4	12.68 ± 0.07	11.73 ± 0.15	122.82 ± 0.17	6.02 ± 0.04	12.69	10.31	84.00	5.17
3	18.24 ± 0.02	1.56 ± 0.18	159.76 ± 0.45	0.67 ± 0.06	18.25	0.95	78.10	0.41
4	21.16 ± 0.04	0.58 ± 0.02	167.16 ± 0.13	0.32 ± 0.01	21.19	0.52	68.00	0.29
3	28.38 ± 0.10	0.01 ± 0.01	16.50 ± 0.26	0.00 ± 0.00	24.79	0.02	84.00	0.01
3	35.58 ± 0.02	7.01 ± 0.08	184.08 ± 0.50	2.95 ± 0.03	35.33	8.69	73.60	3.40
4	37.41 ± 0.08	0.52 ± 0.02	162.36 ± 0.28	0.29 ± 0.01	37.36	0.50	83.00	0.28
4	39.76 ± 0.02	17.98 ± 0.02	193.14 ± 0.36	9.25 ± 0.01	39.67	16.80	88.00	7.94
3	47.82 ± 0.03	16.56 ± 0.16	329.52 ± 0.64	6.90 ± 0.06	47.80	28.23	92.00	9.45
3	51.57 ± 0.02	129.27 ± 0.12	95.13 ± 0.13	23.98± 0.03	51.55	56.57	85.00	14.86
4	54.50 ± 0.04	3.55 ± 0.53	241.76 ± 0.94	1.97 ± 0.19	54.42	2.40	84.00	1.31
4	65.23 ± 0.03	17.11 ± 0.15	360.22 ± 0.65	9.19 ± 0.07	65.15	18.67	77.00	8.45
4	69.01 ± 0.12	1.14 ± 0.06	269.18 ± 0.37	0.64 ± 0.03	68.91	1.10	89.00	0.61
4	72.12 ± 0.03	20.31 ± 0.03	218.50 ± 0.67	10.45± 0.02	71.93	20.44	74.00	9.01
3	-	-	-	-	75.08	0.09	84.00	0.04
4	80.30 ± 0.04	3.69 ± 0.08	1.80 ± 0.24	0.68 ± 0.03	80.10	1.55	82.00	0.85
4	-	-	-	-	83.80	13.51	67.00	6.32
3	84.15 ± 0.07	20.08 ± 0.05	397.93 ± 0.20	10.75± 0.02	84.73	5.60	84.00	2.30
3	85.96 ± 0.32	46.34 ± 0.68	293.48 ± 0.89	24.08± 0.17	85.80	37.37	84.00	11.32
4	93.80 ± 0.03	45.31 ± 0.33	515.19 ± 0.72	23.43± 0.13	93.63	73.78	79.00	21.46

the experimental apparatus and data analysis methodologies are reliable and effective.

5 Usage notes

The obtained dataset presents newly measured cross sections for the ^{165}Ho(n, γ)^{166}Ho reaction studied at the CSNS Back-n facility. Our objective is to comprehensively document the data analysis procedures and make the neutron capture data accessible to both the nuclear physics community and researchers working in related fields for future studies. This dataset has numerous applications in nuclear physics, particularly in the following areas:

(1) The spectroscopic information of heavy nuclei is challenging to obtain experimentally because of the rapid increase in the nuclear level density (NLD) with increasing excitation energies. To address this, statistical models provide a framework for understanding the internal structure of these nuclei at higher energies, relying on key parameters such as the NLD and γ-ray strength function (γSF). These parameters are essential for a wide array of calculations in nuclear reactions, particularly for determining the neutron capture reaction cross sections. The accuracy of these calculations is vital for evaluating the reliability of the nuclear models. In this context, ^{166}Ho, which is an odd–odd deformed nucleus, plays a significant role. The ^{165}Ho(n, γ)^{166}Ho neutron capture reaction is a crucial tool for validating theoretical descriptions of the NLD and γ SF. By examining this reaction, researchers can test and refine the predictive power of nuclear models, thereby enhancing our understanding of the underlying nuclear structures and reaction dynamics.

(2) The nucleosynthesis of elements heavier than iron is considered one of the "11 Biggest Unsolved Mysteries in Physics" that require urgent attention in this century. Nuclear astrophysicists generally agree that slow neutron capture (s-process) and rapid neutron capture (r-process) are the primary mechanisms governing the production of these heavier elements. Holmium, an important rare earth element, is primarily produced through explosive r-process nucleosynthesis, with approximately 9% of its abundance synthesized in the main s-process during the evolution of intermediate-mass stars. The isotope ^{166}Ho is a significant branching nucleus, characterized by a ground-state half-life of 26.9 h and an isomeric state (7^-) with a half-life of 1200 years, primarily formed by the neutron capture of ^{165}Ho. Consequently, the ^{165}Ho(n, γ)^{166}Ho reaction not only depletes the abundance of ^{165}Ho but also influences the abundance of ^{166}Ho and the subsequent

s-process nucleosynthesis products. Therefore, this reaction cross section is critically important for the study of nucleosynthesis in nuclear astrophysics.

(3) Holmium has extensive applications in nuclear medicine, particularly the β^- and γ-emitting isotope ^{166}Ho[$T_{1/2}$=26.9 h, E_β = 1.77 MeV (48%) and 1.85 (51%) MeV, E_γ = 81 keV (6.7%)], which has been developed for radionuclide therapy and single photon emission computed tomography (SPECT) imaging due to its favorable decay properties. The isotope ^{165}Ho is the only naturally stable isotope of Ho (^{nat}Ho) and is used to produce ^{166}Ho through the (n, γ) reaction. Accurate data on the neutron capture cross section and resonance integral for the ^{165}Ho(n, γ)^{166}Ho reaction are essential for evaluating the neutron irradiation time, activity, and yield of ^{166}Ho produced in nuclear reactors.

6 Code availability

Publication of the dataset is accompanied by a software package based on CERN ROOT version 5.34/34 [26], which includes examples for reading the data, generating pulse height spectra of neutrons, performing background subtraction, analyzing neutron resonances, and deriving neutron capture cross sections.

In the dataset, the neutron energy range from 0.2 eV to 2 MeV was logarithmically divided into 3500 bins. The bin intervals and quantities can be reallocated according to a user's range of interest. Two classes, C_6D_6 Data and LiSi Data, are defined to read the corresponding data from the ROOT file. The TChain function was used to read all the ROOT files under the same experimental conditions. For the C_6D_6 data, the neutron energy thresholds were set to E_{dep}^{min} =250 keV and E_{dep}^{max}=7 MeV, with the following detector parameters:

C_6D_6:1 $C_6D_6Data_1$.BCid=1, Min:bin=2822, Max:bin=78865;

C_6D_6:2 $C_6D_6Data_1$.BCid=2, Min:bin=2822, Max:bin=78865;

C_6D_6:3 $C_6D_6Data_1$.BCid=3, Min:bin=2807, Max:bin=78342;

C_6D_6:4 $C_6D_6Data_1$.BCid=4, Min:bin=2890, Max:bin=80629.

For the LiSi data, the signals from eight LiSi detectors were divided into two paths for storage with the following parameters:

LiSi:1 $LiSiData_1$.BCid=5

LiSi:1 $LiSiData_1$.BCid=6

During the in-beam experiment, there was an issue with the second signal from the LiSi detector ($LiSiData_1$.BCid=6). Thus, the first signal ($LiSiData_1$.BCid=5) was selected for data processing. The reaction between neutrons and ^{6}Li primarily generates helium (α) and tritium nuclei (T), resulting in a bimodal structure in the energy spectrum. Owing to the high-energy peak (2.73 MeV) of T, saturation may have occurred during the experiment, leading to a poor statistical performance. Therefore, the α peak was selected as the effective neutron count for the LiSi detector to determine neutron flux. More detailed information related to the data analysis code can be accessed as a notebook in the Science Data Bank, where the complete dataset for this study has been uploaded. A direct link to the dataset is available at https://doi.org/10.57760/sciencedb.21041.

Acknowledgements The authors thank the staff members of the Back-n white neutron facility (https://cstr.cn/31113.02.CSNS.Back-n) at the China Spallation Neutron Source (CSNS) (https://cstr.cn/31113.02.CSNS), for providing technical support and assistance in data collection and analysis. We would like to express thank Hong-Wei Wang, Xi-Chao Ruan, and Jing-Yu Tang for their helpful comments regarding the measurements. We thank Qi-Wen Fan for preparing the samples.

Author Contributions Su-Ya-La-Tu Zhang was involved in conceptualization, methodology, and writing—reviewing and editing. Yong-Shun Huang was responsible for investigation, data curation, and writing—original draft. Wei Jiang, Jie Ren, and Rui-Rui Fan assisted with measurement and methodology. De-Xin Wang carried out formal analysis. Guo-Li and Dan-Dan Niu took measurement. Chun-Lei Zhang participated in editing and English grammar correction. Mei-Rong Huang took part in Writing—reviewing and editing. All authors reviewed the manuscript.

Declarations

Conflict of interest The authors declare that they have no known competing financial interests or personal relationships that could have appeared to influence the work reported in this paper.

References

1. Z.G. Ge, Y.J. Chen, Status and prospects of nuclear data development in China. Chin. Sci. Bull. **60**, 3087 (2015). https://doi.org/10.1360/N972015-00694
2. F. Gunsing, The n_TOF Collaboration, Nuclear data activities at the n_TOF facility at CERN. Eur. Phys. J. Plus **131**, 371 (2016). https://doi.org/10.1140/epjp/i2016-16371-4
3. X.C. Ruan, Progress and prospect of neutron nuclear data measurement. Sci. Sin. Phys. Mech. Astron. **50**, 052002 (2020). https://doi.org/10.1360/SSPMA-2019-0231
4. Z.Q. Chen, Recent progress in nuclear data measurement for ADS at IMP. Nucl. Sci. Tech. **28**, 184 (2017). https://doi.org/10.1007/s41365-017-0335-3
5. S. Zhang, Y.B. Nie, J. Ren et al., Benchmarking of JEFF-3.2, FENDL-3.0 and TENDL-2014 evaluated data for tungsten with 14.8 MeV neutrons. Nucl. Sci. Tech. **28**, 27 (2017). https://doi.org/10.1007/s41365-017-0192-0
6. C. Guerrero, J. Lerendegui-Marco, M. Paul et al., Neutron capture on the s-process branching point ^{171}Tm via time-of-flight and

activation. Phys. Rev. Lett. **125**, 142701 (2020). https://doi.org/10.1103/PhysRevLett.125.142701
7. I. Knapova, A. Couture, C. Fry et al., Photon strength functions, level densities, and isomeric ratio in ^{168}Er from the radiative neutron capture measured at the DANCE facility. Phys. Rev. C **107**, 044313 (2023). https://doi.org/10.1103/PhysRevC.107.044313
8. K. Wisshak, F. Voss, F. Käppeler et al., Stellar neutron capture cross sections of the Lu isotopes. Phys. Rev. C **73**, 015807 (2006). https://doi.org/10.1103/PhysRevC.73.015807
9. C.J. Prokop, A. Couture, S. Jones et al., Measurement of the ^{65}Cu(n, γ) cross section using the detector for advanced neutron capture experiments at LANL. Phys. Rev. C **99**, 055809 (2019). https://doi.org/10.1103/PhysRevC.99.055809
10. J. Tang, R. Liu, G. Zhang et al., Initial years' neutron-induced cross-section measurements at the CSNS Back-n white neutron source. Chin. Phys. C **45**, 062001 (2021). https://doi.org/10.1088/1674-1137/abf138
11. J. Ren, X. Ruan, W. Jiang et al., Neutron capture cross section of ^{169}Tm measured at the CSNS Back-n facility in the energy region from 30 to 300 keV. Chin. Phys. C **46**, 044002 (2022). https://doi.org/10.1088/1674-1137/ac4589
12. S. Zhang, G. Li, W. Jiang et al., Measurement of the ^{159}Tb(n,γ) cross section at the CSNS Back-n facility. Phys. Rev. C **107**, 045809 (2023). https://doi.org/10.1103/PhysRevC.107.045809
13. D.X. Wang, S. Zhang, W. Jiang et al., Resonance analysis of ^{159}Tb(n,γ) reaction based on the CSNS Back-n experiment. Nucl. Sci. Tech. **36**, 43 (2025). https://doi.org/10.1007/s41365-024-01617-9
14. L. Xie, P. Cao, T. Yu et al., Real-time digital trigger system for GTAF-II at CSNS Back-n white neutron source. J. Inst. **16**, P10029 (2021). https://doi.org/10.1088/1748-0221/16/10/P10029
15. Y. Yang, Z. Wen, Z. Han et al., A multi-cell fission chamber for fission cross-section measurements at the Back-n white neutron beam of CSNS. Nucl. Instrum. Methods Phys. Res. A **940**, 486 (2019). https://doi.org/10.1016/j.nima.2019.06.014
16. J.M. Xue, S. Feng, Y.H. Chen et al., Measurement of the neutron-induced total cross sections of ^{nat}Pb from 0.3 eV to 20 MeV on the Back-n at CSNS. Nucl. Sci. Tech. **35**, 18 (2024). https://doi.org/10.1007/s41365-024-01370-z
17. W. Jiang, H.Y. Bai, H.Y. Jiang et al., Application of a silicon detector array in (n, lcp) reaction cross-section measurements at the CSNS Back-n white neutron source. Nucl. Instr. Methods A **973**, 164126 (2020). https://doi.org/10.1016/j.nima.2020.164126
18. J.Y. Tang, Q. An, J.B. Bai et al., Back-n white neutron source at CSNS and its applications. Nucl. Sci. Tech. **32**, 1 (2021). https://doi.org/10.1007/s41365-021-00846-6
19. J.B. Czirr, M.L. Stelts, Measurement of the neutron capture cross section of holmium-165 and gold-197. Nucl. Sci. Eng. **52**, 299 (1973). https://doi.org/10.13182/NSE73-A19477
20. R.L. Macklin, The ^{165}Ho (n,γ) standard cross section from 3 to 450 keV. Nucl. Sci. Eng. **59**, 231 (1976). https://doi.org/10.13182/NSE76-A26821
21. A.D. Carlson, V.G. Pronyaev, D.L. Smith et al., International evaluation of neutron cross section standards. Nucl. Data Sheets **110**, 3215 (2009). https://doi.org/10.1016/j.nds.2009.11.001
22. W.P. Poenitz, Fast neutron capture and activation cross sections. Natl. Bur. Stand.(US), Spec. Publ.(United States) 425, (1975). https://www.osti.gov/biblio/7364993
23. J.H. Gibbons, R.L. Macklin, P.D. Miller et al., Average radiative capture cross sections for 7-to 170-keV neutrons. Phys. Rev. **122**, 182 (1961). https://doi.org/10.1103/PhysRev.122.182
24. J. Voignier, S. Joly, G. Grenier, Capture cross sections and γ-ray spectra from the interaction of 0.5-to 3.0-MeV neutrons with nuclei in the mass range A= 45 to 238. Nucl. Sci. Eng. **112**, 87 (1992). https://doi.org/10.13182/NSE91-92N
25. F. Pogliano, A.C. Larsen, S. Goriely et al., Experimentally constrained ^{165,166}Ho(n,γ) rates and implications for the s-process. Phys. Rev. C **107**, 064614 (2023). https://doi.org/10.1103/PhysRevC.107.064614
26. R. Brun, F. Rademakers, ROOT-an object oriented data analysis framework. Nucl. Instr. Methods A **389**, 81 (1997). https://doi.org/10.1016/S0168-9002(97)00048-X
27. Q. Li, G. Luan, J. Bao et al., The ^{6}LiF-silicon detector array developed for real-time neutron monitoring at white neutron beam at CSNS. Nucl. Instr. Methods A **946**, 162497 (2019). https://doi.org/10.1016/j.nima.2019.162497
28. Y. Chen, G. Luan, J. Bao et al., Neutron energy spectrum measurement of the Back-n white neutron source at CSNS. Eur. Phys. J. A **55**, 115 (2019). https://doi.org/10.1140/epja/i2019-12808-1
29. Q. Wang, P. Cao, X. Qi et al., General-purpose readout electronics for white neutron source at China Spallation Neutron Source. Rev. Sci. Instrum. **89**, 013511 (2018). https://doi.org/10.1063/1.5006346
30. J. Ren, X. Ruan, W. Jiang et al., Background study for (n, γ) cross section measurements with C_6D_6 detectors at CSNS Back-n. Nucl. Instrum. Methods Phys. Res. A **985**, 164703 (2021). https://doi.org/10.1016/j.nima.2020.164703
31. S. Agostinelli, J. Allison, K. Amako et al., GEANT4-a simulation toolkit. Nucl. Instrum. Methods Phys. Res. A **506**, 250 (2003). https://doi.org/10.1016/S0168-9002(03)01368-8
32. U. Abbondanno, G. Aerts, H. Alvarez et al., New experimental validation of the pulse height weighting technique for capture cross-section measurements. Nucl. Instrum. Methods Phys. Res. A **521**, 454 (2004). https://doi.org/10.1016/j.nima.2003.09.066
33. G.L. Yang, Z.D. An, W. Jiang et al., Measurement of Br(n,γ) cross sections up to stellar s-process temperatures at the CSNS Back-n. Nucl. Sci. Tech. **34**, 180 (2023). https://doi.org/10.1007/s41365-023-01337-6
34. N.M. Larson, Updated user's guide for Sammy: Multilevel R-matrix fits to neutron data using Bayes' equations[R]. Oak Ridge National Lab.(ORNL), Oak Ridge, TN (United States), (2008). https://doi.org/10.2172/941054
35. B. Jiang, J. Han, W. Jiang et al., Monte-Carlo calculations of the energy resolution function with Geant4 for analyzing the neutron capture cross section of ^{232}Th measured at CSNS Back-n. Nucl. Instrum. Methods Phys. Res. A **1013**, 165677 (2021). https://doi.org/10.1016/j.nima.2021.165677
36. M.B. Chadwick, M. Herman, P. Oblozinsky et al., ENDF/B-VII.1 nuclear data for science and technology: cross sections, covariances, fission product yields and decay data. Nucl. Data Sheets **112**, 2887 (2011). https://doi.org/10.1016/j.nds.2011.11.002
37. A.D. Carlson, V.G. Pronyaev, R. Capote et al., Evaluation of the neutron data standards. Nucl. Data Sheets **148**, 143 (2018). https://doi.org/10.1016/j.nds.2018.02.002
38. A.J. Koning, D. Rochman, J.C. Sublet et al., TENDL: complete nuclear data library for innovative nuclear science and technology. Nucl. Data Sheets **155**, 1 (2019). https://doi.org/10.1016/j.nds.2019.01.002